

REPETITIVE ALL SOLID-STATE PULSE MARX TYPE GENERATOR WITH ENERGY RECOVERY CLAMP CIRCUIT FOR INDUCTIVE LOADS*

L. M. Redondo^{1,2,ξ} M. T. Pereira³

¹*Instituto Superior de Engenharia de Lisboa ISEL/CEEL, Rua Conselheiro Emídio Navarro 1, Lisbon, Portugal*

²*Centro de Física Nuclear da Universidade de Lisboa, Portugal*

³*Lusoforma Comércio e Indústria de Embalagens, S.A., Rua do Mercado, S. Carlos, Mem Martins, Portugal*

Abstract

A newly developed Marx type circuit topology that achieves both output-voltage multiplication and energy recovery, which has been developed for inductive load applications, namely Electromagnetic metal Forming (EMF), based on an all-solid-state Marx type generator, is described.

The proposed circuit takes advantage on the power semiconductor switches intensive use, replacing the conventional Marx Bank passive elements, to increase the performance, strongly reducing losses and increasing the pulse repetition frequency. Additionally, the generator is designed with an energy reset circuit that enables the use of inductive loads, recovering the inductive energy during the semiconductor switches off-state, back to the energy storage capacitors. Preliminary results from this EMF modulator prototype are presented and discussed.

I. INTRODUCTION

In the last decade, repetitive high-voltage pulses have been used extensively in industrial applications, like Food Sterilization and Surface Engineering, which increased the need of efficient, flexible and suitable power supplies, based on solid-state switches [1, 2].

To deal with this, a number of techniques have been used in order to generate high-voltage pulses from generators with optimised performance and characteristics, taking the best of solid-state technology, regarding the fact that semiconductors are still, compared with hard-tube switches, relatively low power devices, and very sensitive to voltage and current instabilities, needing auxiliary protection circuits.

Due to its innovation, it's worth mention the techniques based on power-electronic circuit topologies that were developed for switching power supplies, which with different operating conditions and small circuit changes were adapted for high-voltage pulsed generation [3, 4].

Also recent is the important technological upgrading done in the mature Marx generator concept that as has been intensively used through the years, in order to increase the performance of the original circuit [5, 6].

Nowadays, one of the most challenging pulse power application is Electromagnetic Metal Forming (EMF), where electromagnetic forces are used to form metal in two very broad implementations, radial and sheet forming [7].

Briefly, EMF works by the magnetic induction effect. When a coil or solenoid is placed near a metallic conductor and pulsed (kV and kA), a magnetic field is generated between the coil and the workpiece. If done quickly enough, the magnetic field is excluded from penetrating into the workpiece for a short period of time. During this time, a pressure is generated on the workpiece that is proportional to the magnetic flux density squared. This "magnetic" pressure is what provides the forming energy. The energy is usually supplied to the workpiece in the form of kinetic energy. The magnetic pressure pulse accelerates the workpiece up to a certain velocity (such as 200-300 m/s). This kinetic energy drives the material into the die, causing forming on impact [7].

We will report on a newly developed all-solid-state Marx type circuit topology, to achieve both output-voltage multiplication and energy recovery, developed for inductive load applications, in particular EMF.

In this circuit, the conventional passive elements that were present in the original Marx Bank generator, for charging the energy storing capacitors and limit their self-discharge current during the pulse period, were replaced by power semiconductors, diodes and IGBTs (Isolated Gate Bipolar Transistors), used intensively, in order to increase the performance, strongly reducing losses and increasing the pulse repetition frequency.

Additionally, the generator is designed with an energy reset circuit that enables the use of inductive loads, recovering the inductive energy during the power semiconductors off-state, back to the energy storage capacitors. This decreases the charging time, and enables higher frequency operation, increasing the pulse generator yield.

Preliminary experimental high-voltage measurements, voltage and current, taken from an assembled prototype will be presented and compared with the results of circuit simulations. This will assist the discussion on circuit performance and launch hints for further improvements, to construct an industrial modulator.

* Work supported by ISEL and Lusoforma S.A. under a scientific contract.

ξ email: lmredondo@deea.isel.ipl.pt

II. CIRCUIT DESCRIPTION

Fig. 1 shows a simplified schematic of the Marx type pulse modulator, with n stages, for delivering repetitive negative high-voltage rectangular pulses to a resistive/capacitive, R_l/C_l , type of load. This modular circuit, proposed by [5] to increase the performance of the classic Marx modulator topology, uses in each stage an energy storing capacitor C_i , a diode D_{ci} and two power transistors (T_{ci} and T_{di}), where the subscript $i \in \{1, \dots, n\}$. During the capacitor C_i charging period, T_{ci} are *on* and T_{di} are *off*. After that, during pulse period, T_{di} are *on* and T_{ci} are *off* [5].

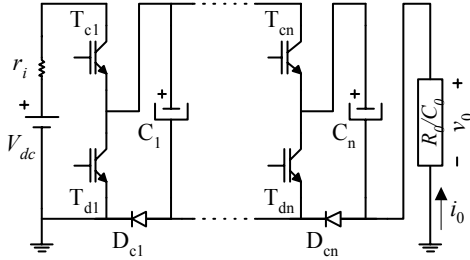


Figure 1. Marx type modulator for delivering negative high-voltage pulses to resistive/capacitive loads [5].

The circuit topology presented in Fig. 1 can be modified to include an alternative path to the load current, i_0 , when connected to an inductive load, L_0 , after the pulse period, as shown in Fig. 2.

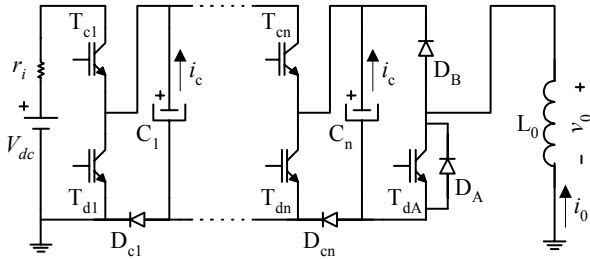


Figure 2. Marx type pulse modulator for delivering negative high-voltage pulses to inductive loads.

Considering the circuit in Fig. 1, the circuit in Fig. 2 presents an additional semiconductor switch, T_{dA} , and two extra diodes, D_A e D_B .

These results on adding an extra half-bridge arm to the circuit, where the top switch can be substituted by a diode and the bottom one must be a power transistor with a freewheeling diode.

The operation of Fig. 2 circuit can be understood, considering only three different operating modes, with the simplified theoretical waveforms shown in Fig. 4. In the first mode, Fig. 3 (a), switches T_{ci} and T_{di} (and T_{dA}) are, respectively, *on* and *off*. During this period, t_c , capacitors C_i are charged, with total energy, approximately, equal to

$$E_{cap} = n0.5C_iV_{dc}^2, \quad (1)$$

considering that ideally all capacitors are charged with the power supply voltage V_{dc} .

During this mode, diode D_A is *on*, ensuring that the voltage applied to the load is roughly zero, as seen in Fig. 4 (c). The circuit parameters and operating conditions guaranty, also, that the charging current is insignificant when compared with the load current in order to reduce the power supply load and size, Fig. 4 (e).

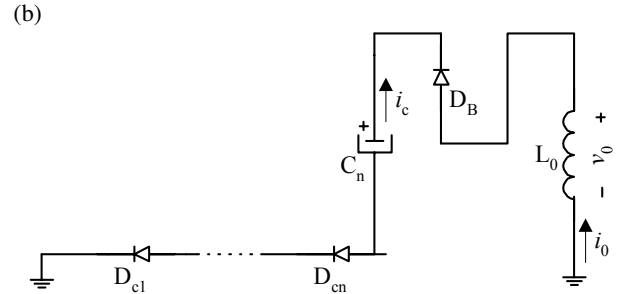
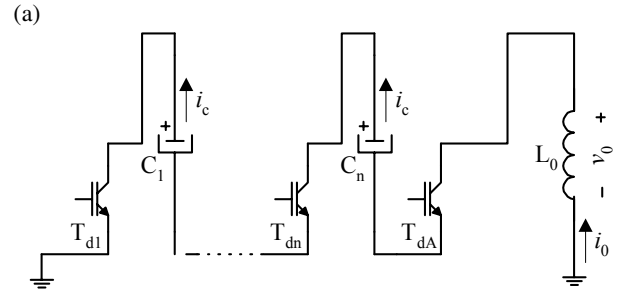
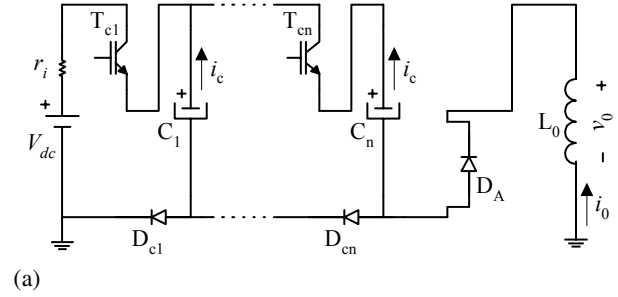


Figure 3. (a) Charging mode; (b) Pulse mode and (c) Energy recovery mode, for Fig. 2 circuit operation.

In the second operating mode, Fig. 3 (b), switches T_{ci} and T_{di} (and T_{dA}) are, respectively, *off* and *on*. During this period, t_p , capacitors C_i are connected in series and the voltage applied to the load, v_0 , is, approximately, equal to,

$$v_0 = -nV_{dc}. \quad (2)$$

Considering an LC ideal circuit, the current i_0 is equal to,

$$i = \frac{V_c}{\omega_0 L_0} \text{sen} \omega_0 t, \quad (3)$$

where

$$\omega_0 = \frac{1}{\sqrt{L_0 C_c}}, \quad (4)$$

is the natural oscillating frequency. Hence, if there are no dissipative elements in the current circuit path, the maximum i_0 current, in L_0 , could be determined by

$$I_0 = V_c \sqrt{\frac{C_c}{L_0}}, \quad (5)$$

corresponding to a time when the entire energy store in the capacitors C_i , given by (1), was delivered to the inductance L_0 (load), and the capacitors voltage is zero.

In this circuit, according to Fig. 4 (d) and (e), the current in the load is switch-off before it reaches its maximum (5). This is done in order to get a short current pulse (dozens of microseconds) to the load.

In the third operating mode, Fig. 3 (c), switches T_{ci} and T_{di} (and T_{da}) are *off*. During this period, t_r , the voltage applied to the load L_0 is, roughly, V_{dc} (Fig. 4 c)) and current i_0 has a path through D_B . The energy is sent back to the energy storage capacitors, C_i , until $i_0=0$. The capacitor with the lowest voltage receives this current, Fig. 4 (e), which increases the capacitor energy.

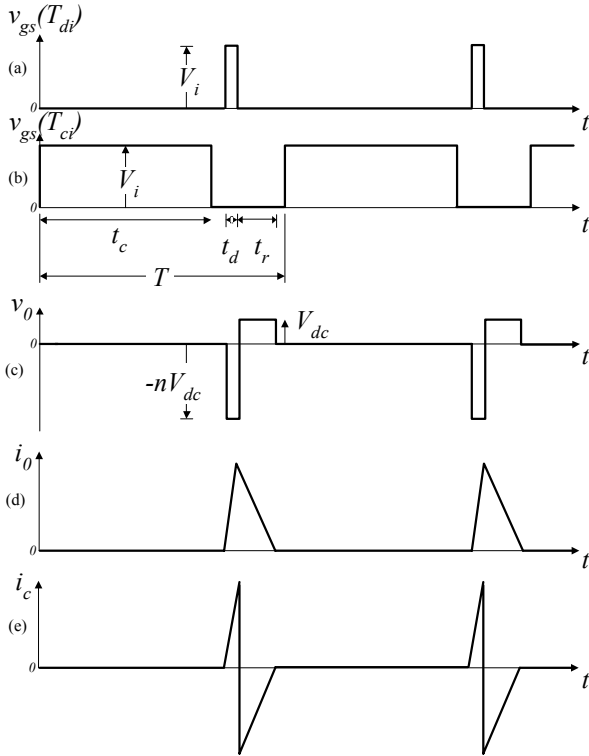


Figure 4. Theoretical waveforms for Fig. 2 circuit operation: (a) T_{di} drive signal; (b) T_{ci} drive signal; (c) load voltage, v_p ; (d) load current, i_0 ; (e) capacitor C_i current, i_c .

Considering the power supply voltage constant, V_{dc} , the reset voltage is always the same (voltage in each capacitor), independent on the number of stages in the

Marx generator. However, increasing the number of stages, the pulse voltage is higher and so the reset time t_r is longer, to guarantee that the energy is equal, Fig. 4 (c), during the pulse and during the reset period.

Taking into account Fig. 4 (c), after the reset time, t_r , i_0 goes to zero and diodes are off. The voltage applied to the load is zero, after which the first operation mode begins again, Fig. 3 (a).

Regarding the drive signals, Fig. 4 (a) and (b), $v_{gs(T_{di})}$ and $v_{gs(T_{ci})}$, respectively, of semiconductors T_{di} and T_{ci} , Fig. 2 circuit is more complex than Fig. 1 circuit. Due to the reset period the drive signals to switches T_{ci} must be delayed by t_r , as can be seen in Fig. 4 (b). This difference creates extra complexity for the semiconductors drives.

In both circuits, the semiconductors must be driven synchronously, and as all the switches are at different potentials, it is required gate circuits with galvanic isolation (optical fibres are used to transmit the gate signals).

III. RESULTS AND DISCUSSION

Fig. 5 shows the implemented EMF prototype circuit based on Fig. 2 circuit. In this case, only one stage was assembled due to the fact that the semiconductors blocking voltage was higher than the power supply voltage, V_{dc} . The circuit was assembled with a 1000 $\mu\text{F}/2000\text{V}$ capacitor C_e (with about 150 nH equivalent series inductance), Eupec FD1200R17KE3-K_B2, solid-state switches, T_1/D_1 and T_2/D_2 that are the ones that handled the high-currents. T_1 IGBT is a low current device. The load was a 18 μH and 0.01 Ω coil. The first results were taken for $V_{dc}=100$ V, $r_i=100$ Ω with 10 Hz repetition rate and 0.06 % duty cycle.

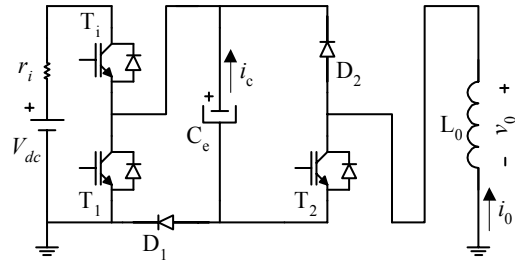


Figure 5. Assembled EMF prototype modulator circuit.

Fig. 6 shows, respectively, the simulation results for v_0 , i_0 and i_c , considering the circuit in Fig. 5 with a 5 nF parasitic capacitance in parallel with the load. This capacitance represents mainly the L_0 coil windings equivalent distributed capacitance.

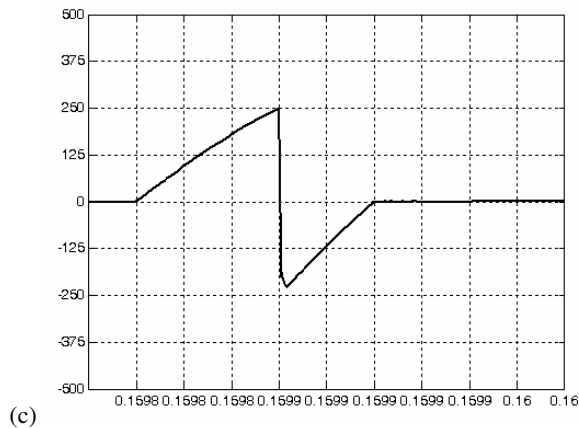
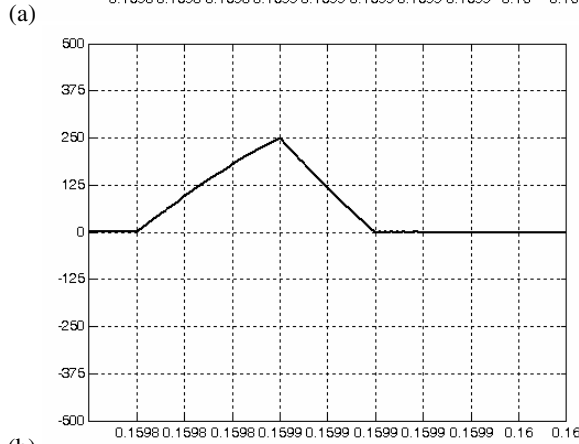
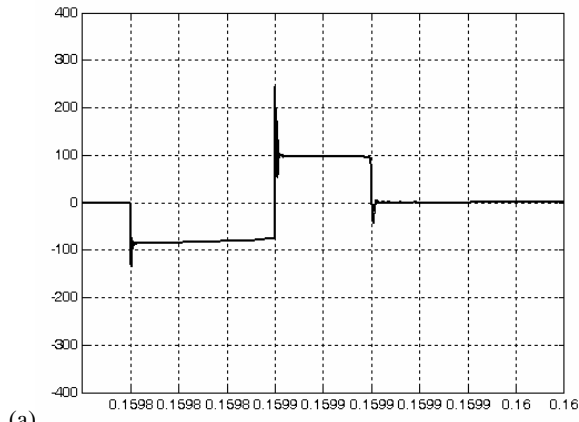


Figure 6. Fig. 5 circuit simulation results for, 20 $\mu\text{s}/\text{div}$: v_o , 100 V/div; i_o 125 A/div; i_c 125 A/div.

Fig. 8 shows, respectively, the experimental measured values for the load voltage v_o , load current i_o and capacitor current i_c for Fig. 5 circuit. For the applied 100 V, the current increases during $t_d=60 \mu\text{s}$, up to 250 A, and then is reset, with -100 V, during $t_r=40 \mu\text{s}$. The reset period is lower than the pulse period due to the energy losses in the circuit resistances. During the reset period the current i_o is returned back to the capacitor C_c , as can be seen on Fig. 7 (c).

The results show overshoot and ringing, mainly in the output voltage v_o , and more intense during the second to the third operation mode switching.

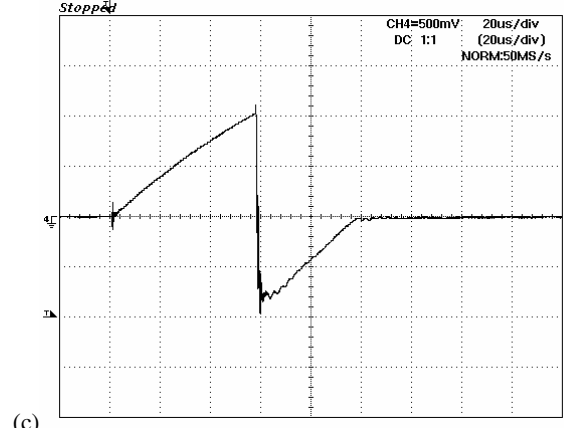
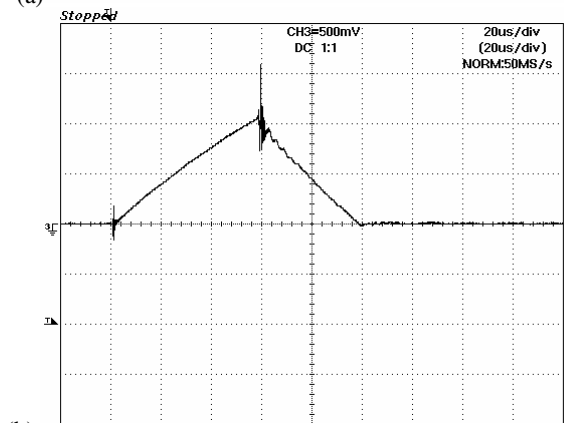
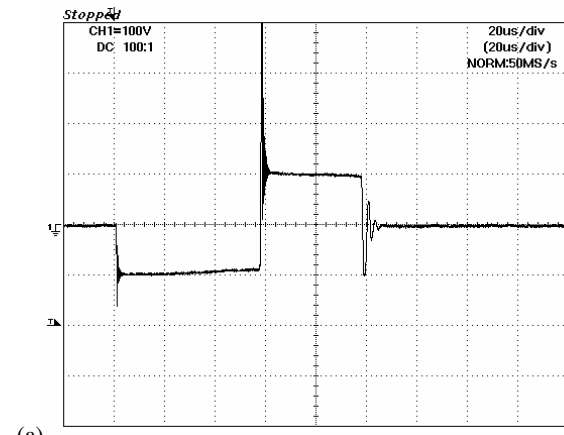


Figure 7. Fig. 5 circuit experimental results for, 20 $\mu\text{s}/\text{div}$: v_o , 100 V/div; i_o 125 A/div; i_c 125 A/div.

The resonance between the equivalent series inductance (ESL), of the main capacitor, with the parasitic distributed capacitances is the main cause for these instability. To limit these and to protect the semiconductors, RC protection circuits (i.e. snubbers) were placed in parallel with the semiconductors. However, this was not enough and a more careful assemble is due. Also, the main capacitor must be replaced by one with lower ESL. Nevertheless, the results are promising and most important the simulation and theoretical results agree with the experimental results.

IV. CONCLUSION

A new all-solid-state Marx type circuit topology for inductive pulsed power applications was successfully presented. With this circuit, both output-voltage multiplication and inductive energy recovery back to the energy storing capacitors is possible.

The proposed generator is designed with an energy reset circuit that enables the use of inductive loads, recovering the inductive energy during the power semiconductors off-state, back to the energy storage capacitors. This decreases the charging time, and enables higher frequency operation, increasing the pulse generator yield. In this circuit, the intensive use of power semiconductors, diodes and IGBTs (Isolated Gate Bipolar Transistors), also increases the performance, compared to the traditional Marx generator, strongly reducing losses and increasing the pulse repetition frequency.

Preliminary experimental results of an Electromagnetic Metal Forming modulator prototype were presented and compared with the results of circuit simulations. The agreement was good. Nevertheless, there are still some improvements due in order to reduce the overshoot and ringing if an industrial modulator is to be assembled.

V. REFERENCES

- [1] M.P.J. Gaudreau, T. Hawkey, J. Petry and M. Kempkes, "A solid state pulsed power system for food processing," in *Proceed. Pulsed Power Plasma Science*, 2001, vol. 2, pp. 1174-1177.
- [2] D.M. Goebel, "Pulse Technology", Chapter 8 de "Handbook of Plasma Immersion Ion Implantation & Deposition," Editor Anders, André, 1st edition, John Wiley & Sons, New York, 2000, p. 760, ISBN 0-471-24698-0.
- [3] Tian *et al.*, "Special modulator for high frequency, low-voltage plasma immersion ion implantation," *Review of Scientific Instruments*, vol. 70, no. 3, Mar. 1999, pp. 1824-1828.
- [4] L.M. Redondo, N. Pinhão, E. Margato, and J. Fernando Silva, "Progress on high-voltage pulse generators, using low voltage semiconductors (<1 kV), designed for plasma immersion ion implantation (PIII)," *Surf. Coat. Technol.*, Vol. 156, pp. 61-65, 2002.
- [5] L. M. Redondo, J. Fernando Silva, P. Tavares and E. Margato, "All Silicon Marx-bank topology for high-voltage, high-frequency rectangular pulses," in *Proc. 2005 IEEE 36th Annual Power Electronics Specialists Conference*, p. 1170.
- [6] J.-H. Kim, M.-H. Ryu, B.-D. Min, S.V. Shenderoy, J.-S. Kim and G.-H. Rim, "High voltage pulse power supply using Marx generator & solid-state switches," in *Proc. Industrial Electronics Society, 2005. IECON 2005, 31st Annual Conference of IEEE*, p. 1244.
- [7] A. Meriched, M. Féliachi and H. Mohellebi, "Electromagnetic Forming of Thin Metal Sheets," *IEEE Transactions on Magnetics*, vol. 36, no. 4, July 2000.